

Associate Everything Detected: Facilitating Tracking-by-Detection to the Unknown

Zimeng Fang, Chao Liang, Xue Zhou, Shuyuan Zhu, and Xi Li

Abstract—Multi-object tracking (MOT) emerges as a pivotal and highly promising branch in the field of computer vision. Classical closed-vocabulary MOT (CV-MOT) methods aim to track objects of predefined categories. Recently, some open-vocabulary MOT (OV-MOT) methods have successfully addressed the problem of tracking unknown categories. However, we found that the CV-MOT and OV-MOT methods each struggle to excel in the tasks of the other. In this paper, we present a unified framework, Associate Everything Detected (AED), that simultaneously tackles CV-MOT and OV-MOT by integrating with any off-the-shelf detector and supports unknown categories. Different from existing tracking-by-detection MOT methods, AED gets rid of prior knowledge (e.g. motion cues) and relies solely on highly robust feature learning to handle complex trajectories in OV-MOT tasks while keeping excellent performance in CV-MOT tasks. Specifically, we model the association task as a similarity decoding problem and propose a sim-decoder with an association-centric learning mechanism. The sim-decoder calculates similarities in three aspects: spatial, temporal, and cross-clip. Subsequently, association-centric learning leverages these threefold similarities to ensure that the extracted features are appropriate for continuous tracking and robust enough to generalize to unknown categories. Compared with existing powerful OV-MOT and CV-MOT methods, AED achieves superior performance on TAO, SportsMOT, and DanceTrack without any prior knowledge. Our code is available at <https://github.com/balaboooo/AED>.

Index Terms—Multi-object tracking, association, open vocabulary, attention mechanism, tracking-by-detection.

I. INTRODUCTION

Closed-vocabulary multi-object tracking (CV-MOT) methods [1]–[5] are designed to track a predefined, limited set of target classes consistent with training data. They have achieved remarkable results in CV-MOT datasets [6]–[9]. Nevertheless, some practical applications like autonomous driving and augmented reality (AR) require trackers to handle new or unexpected classes. CV-MOT methods cannot expand the categories during the detection phase. In contrast, with the help

of zero-shot capability of Multimodal Large Language Model (MLLM) [10]–[12], open-vocabulary multi-object tracking (OV-MOT) methods [13]–[15] can adapt to a broader range of categories, including unseen ones in training. However, when tracking certain categories, OV-MOT methods are less effective than well-finetuned CV-MOT methods.

To unify CV-MOT and OV-MOT within a single framework, we reformulate the tracking task to associate arbitrary detections under the tracking-by-detection paradigm. We intend to build our framework based on the “Associate Everything Detected” concept and name our method AED which offers plug-and-play compatibility with various off-the-shelf detectors. AED is trained on certain categories and aims to associate arbitrary detections including unseen categories. Therefore, a robust association method capable of handling complex matching and long-term ID preservation is crucial for MOT.

According to whether to use appearance features during association, existing tracking-by-detection MOT methods can be classified into two main categories: appearance-independent and appearance-based.

1) Appearance-independent methods [1], [16], [17] fully utilize prior knowledge to achieve state-of-the-art performance in CV-MOT scenarios [7]–[9] (Fig. 1(a)). For example, with high intersection over union (IoU) of objects between adjacent frames, most of these methods operate under the implicit assumption that objects have minimal movement between the two frames. Additionally, some of them also rely on motion or other prior knowledge, e.g., linear movement [18] and consistent height and confidence variation of objects [19]. However, the reliance on prior knowledge is disastrous in the OV-MOT setting where the motion patterns of different categories exhibit considerable variability. It is difficult to model these complex motion patterns by using prior knowledge.

2) Some appearance-based methods [2], [4], [20] leverage the learned re-identification (ReID) features to compensate for the drawback of appearance-independent methods in CV-MOT (Fig. 1(b)). In particular, besides using prior knowledge, they train their appearance models or branches following the ReID learning pipeline (e.g. classification or triplet supervision [21]). Other methods [13], [14], [22] (Fig. 1(c)), especially for OV-MOT methods, use dual contrastive learning strategy for feature learning between two frames. However, the learning objectives of both ReID-based and dual contrastive-based methods are inconsistent with the inference objectives of the association stage for MOT. The association in MOT requires temporal discriminability, while ReID-based methods enable the model to have highly global identity (ID) discriminability by unsuitably modeling the association problem as a classifica-

This work has been submitted to the IEEE for possible publication. Copyright may be transferred without notice, after which this version may no longer be accessible.

Zimeng Fang and Chao Liang contributed equally to this work; Corresponding authors: Xue Zhou and Xi Li.

Zimeng Fang and Chao Liang are with the School of Automation Engineering, University of Electronic Science and Technology of China (UESTC), Chengdu 611731, China; E-mail: {fangzimeng, 201921060415}@std.uestc.edu.cn.

Xue Zhou is with the Shenzhen Institute of Advanced Study and the School of Automation Engineering, University of Electronic Science and Technology of China (UESTC), Shenzhen 518110, China; E-mail: zhouxue@uestc.edu.cn.

Shuyuan Zhu is with the School of Information and Communication Engineering, University of Electronic Science and Technology of China (UESTC), Chengdu 611731, China; E-mail: eezsy@uestc.edu.cn.

Xi Li is with the College of Computer Science and Technology, Zhejiang University, Hangzhou 310027, China; E-mail: xilizju@zju.edu.cn.

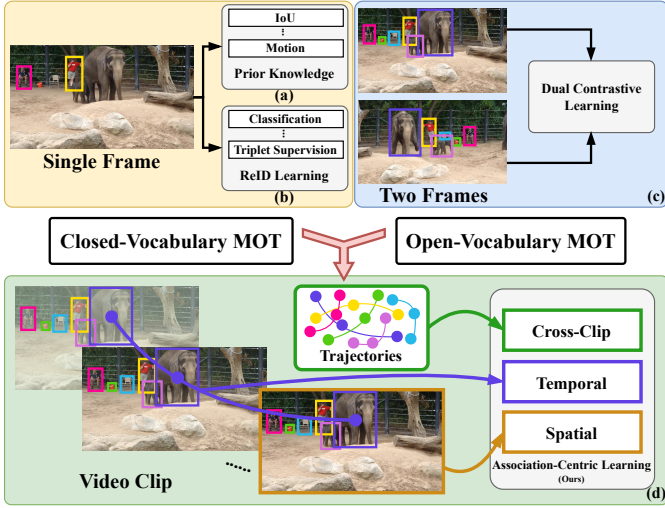


Fig. 1. Motivation of AED. Existing closed-vocabulary and open-vocabulary trackers focus on tracking certain categories (e.g. person) and arbitrary categories (e.g. person, elephant, chair, bucket, etc) respectively. For the association phase, (a) appearance-independent methods rely on prior knowledge; (b) some appearance-based CV-MOT methods train their appearance branch following the ReID pipeline; (c) some other appearance-based methods use dual contrastive strategy for feature learning; (d) our proposed method unifies CV-MOT and OV-MOT tasks and uses association-centric learning.

tion or alignment task within feature space. Dual contrastive-based methods lack temporal diversity, i.e., the association stage of MOT usually needs to handle intricate associations across far more than two frames. We argue that ignorance or lack of association-driven learning may lead to ambiguity during training.

Based on the above analysis, we need to address two key issues to accommodate both CV-MOT and OV-MOT. 1) **Prior Knowledge Reliance**: To minimize the reliance on prior knowledge and simplify the tracking logic, we only use appearance cues and model the association task in MOT as the similarity decoding problem. Specifically, we design a similarity decoder (sim-decoder) where we model the objects in the current frame as object queries and historical trajectories as track queries. Then we use the sim-decoder to decode the similarities between object queries and track queries. Without any prior knowledge, the similarity is then used for association directly. Due to the sufficient reliability of the sim-decoder, we do not employ any complex trajectory initialization strategies during association. 2) **Association-Learning Ignorance**: To solve this problem, we propose an association-centric learning mechanism, along with the sim-decoder, to explore training data in three aspects: spatial, temporal, and cross-clip, as illustrated in Fig. 1(d). Particularly, contrastive learning is utilized for all three of the aspects above. Spatial contrastive learning distinguishes IDs within a single frame to lay the groundwork for temporal association. Temporal contrastive learning matches current frame detections to historical trajectories to exhibit better temporal ID consistency. Furthermore, cross-clip contrastive learning enhances long-term ID consistency among different short trajectories.

We summarize our contributions as follows:

- We propose a unified association-driven tracking-by-

detection MOT framework to associate every detected object, bridging the gap between CV-MOT and OV-MOT.

- We design a sim-decoder followed by an association-centric learning mechanism to decode highly robust similarities and ensure that the learned features are more appropriate for tracking.
- Extensive experiments demonstrate that our method effectively improves the performance in both OV-MOT and CV-MOT tasks, especially in scenarios involving large movements, severe occlusions, similar appearances, and low frame rates.

II. RELATED WORKS

In this section, we first briefly review the two most prevailing MOT paradigms, tracking-by-detection and tracking-by-query. Then we review some related works of Open-Vocabulary MOT.

A. Tracking-by-Detection MOT

In the past few years, tracking-by-detection has been a popular and high-performance paradigm for CV-MOT tasks. Objects are first detected and then associated. Guided by this, many methods have introduced innovative approaches in various aspects, such as motion features [1], [16], [17], [19], [23], appearance features [2], [20], and the real-time performance [3], [4] of the algorithms. SORT [1] introduces a Kalman filter [18] to predict the most probable location of objects in the next frame, which effectively solves the association problem. Based on SORT, DeepSORT [2] uses an extra re-identification (ReID) model to compensate for the shortcomings of IoU (Intersection over Union) distance. JDE [3] modifies Yolov3 [24] to simultaneously output detection results and ReID features. CStrack [4] finds the competition between detection and ReID and further proposes a reciprocal network to learn task-dependent representations. ByteTrack [16] uses a simple but effective strategy to recover the true positive boxes with low confidence scores. However, these tracking-by-detection algorithms heavily rely on prior knowledge, especially motion cues (e.g. IoU distance). Some other advanced methods [17], [19], [20], [23] design handcrafted tracking logic (e.g. observation re-update and iterative scale-up IoU) to adapt to specific tracking scenarios such as dancing [9], pedestrian walking [7], [8], and sports [25]. These handcrafted tracking logics are not conducive to open-vocabulary tracking because motion patterns are hard to describe in scenarios with numerous categories. The reliance on handcrafted tracking logic significantly harms their universality in diverse scenarios.

B. Tracking-by-Query MOT

Recently, transformer [26] has shown its exceptional performance on a wide range of tasks. Queries of the transformer can aggregate specific features according to different preferences. Based on this, some existing MOT methods [5], [27], [28] model a trajectory as a query or a set of queries. Some other tracking-by-query methods [29], [30] use the attention mechanism [26] to aggregate temporal information. Then they

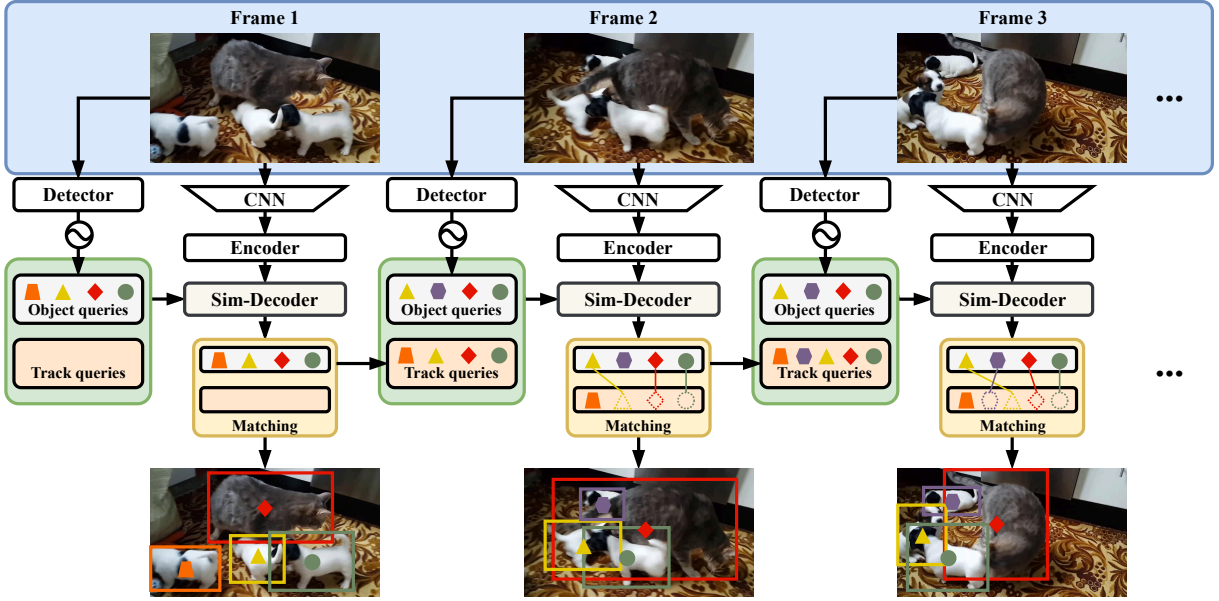


Fig. 2. Overview of AED. During inference, a replaceable detector outputs boxes of arbitrary categories (e.g. cat and dog), and boxes are encoded into object queries. A CNN and a transformer encoder are responsible for extracting features of the frame. The sim-decoder calculates the similarities between object queries and track queries. Similarities are then used for matching. If a track query is matched (dashed lines), it will be updated by its object query. Matching results will be the track queries for the next frame.

use queries to detect and track targets across frames end-to-end. MOTR [31] advances Deformable DETR [32] into a query-based MOT tracker. MOTRv2 [33] improves the detection performance of MOTR by introducing an additional detector. These trackers are highly integrated. However, such advantages can also be considered as their shortcomings somehow. Their parameters, including queries, are highly category-related, and they are unable to track unseen categories. ColTrack [28] leverages multiple historical queries of the same ID to become frame-rate-insensitive. However, multiple queries add computational burden, and ColTrack also struggles to perform tracking for unknown categories.

C. Open-Vocabulary MOT

With the advancement of the MOT community, various MOT datasets [7]–[9] have abundant scenarios and a variety of motion patterns. However, these datasets predominantly feature the person category, which is not in accord with the practical and universal scenario. To address this problem, OV-MOT aims to track unseen categories. Unfortunately, very few papers have tackled the OV-MOT problem. Li et al. [13] first define the task of OV-MOT and propose OVTrack to handle this problem on the TAO [34] dataset. Different from classical CV-MOT (i.e. the categories for testing and training are consistent), OV-MOT splits categories of objects into non-overlapped $\mathcal{C}^{\text{base}}$ and $\mathcal{C}^{\text{novel}}$. Only $\mathcal{C}^{\text{base}}$ is used for training and $\mathcal{C}^{\text{base}}$ together with $\mathcal{C}^{\text{novel}}$ are then used for testing by given names of the novel categories. OVTrack leverages distilled knowledge from CLIP [10] to track unseen categories $\mathcal{C}^{\text{novel}}$. Moreover, it employs a contrastive learning approach to distinguish different IDs. By integrating 10 million automatically labeled data, GLEE [14] uses a unified framework to address several open-vocabulary tasks like detection, segmentation, grounding,

tracking, etc. However, these methods overlook the true needs of the model during the association process leading to their suboptimal performance. NetTrack [15] leverages fine-grained features, i.e., point-level visual cues, to track highly dynamic objects. Nevertheless, its association performance is still less than ideal in some extremely dynamic scenarios like TAO.

III. METHOD

In this section, we introduce AED that aims to Associate Everything Detected. Given arbitrary detection results, it can track objects in both closed and open vocabulary scenarios. It contains two key components: similarity decoder (sim-decoder) and association-centric learning mechanism. We first give an overview of AED in Section III-A, and then introduce sim-decoder and association-centric learning mechanism in Section III-B and Section III-C respectively. In Section III-D, we provide some training details of AED.

A. Overview

We give an overview of AED in Fig. 2. We build AED upon the tracking-by-detection paradigm for two reasons. On the one hand, detection results can be arbitrary objects of any category during inference, which is the fundamental precondition of AED. On the other hand, AED can be applied plug-and-play to any object detectors.

We design AED to decode similarities between detection results and historical trajectories and perform matching. The input of AED is a video sequence. For every frame, there is an object detector (e.g., Co-DETR [35], YOLOX [36] or RegionCLIP [11]) outputting bounding boxes and a CNN backbone (i.e., ResNet50 [37]) followed with an encoder [32] extracting image features. For every frame, we encode the

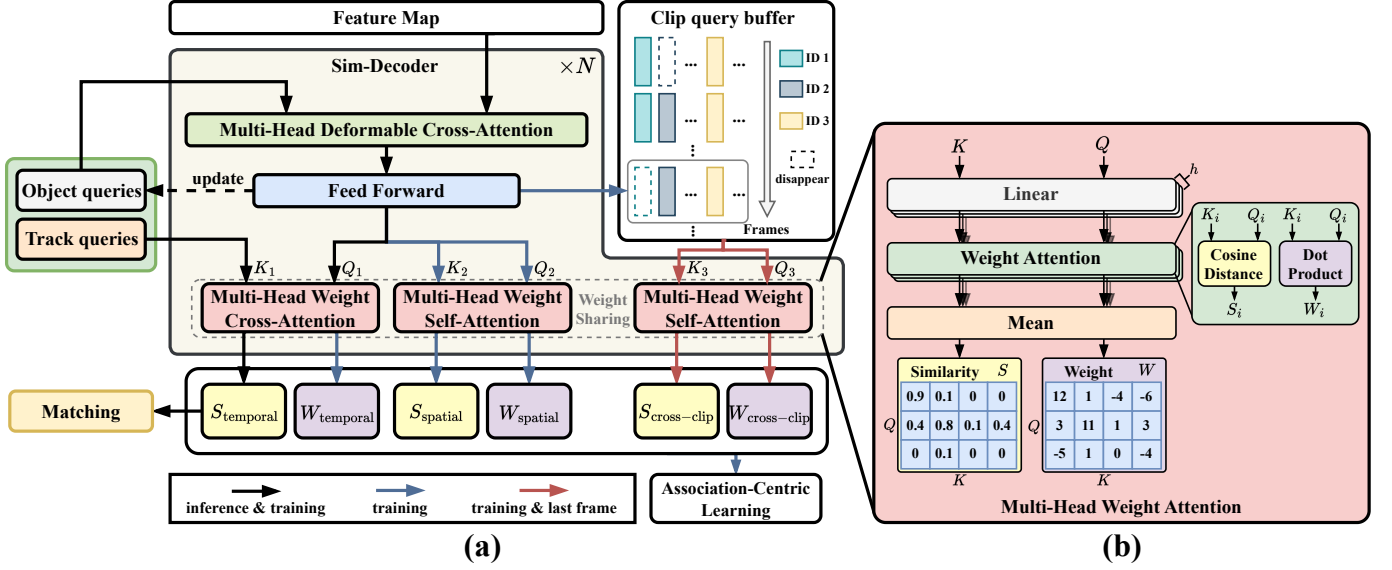


Fig. 3. Design of (a) similarity decoder (sim-decoder) and (b) multi-head weight attention. Object queries and feature maps of the frame are fed into multi-head deformable cross-attention to extract features of objects. Then, the feed-forward network updates the object queries. Residual connection is omitted for simplicity. We use a multi-head weight cross-attention to calculate temporal similarities S_{temporal} , which is then used for matching. During training, we use three multi-head weight attentions with shared weights to get temporal similarities S_{temporal} and weights W_{temporal} , spatial similarities S_{spatial} and weights W_{spatial} , and cross-clip similarities $S_{\text{cross-clip}}$ and weights $W_{\text{cross-clip}}$ respectively. These three similarity and weight matrices are then used for the association-centric learning mechanism.

detected boxes into object queries. Therefore, we regard the detections as object queries and the existing trajectories as track queries of the current frame. Then the object queries and track queries are fed into a novel sim-decoder (Section III-B) to decode their similarities. To minimize the reliance on prior knowledge and adapt to the vast majority of motion patterns, AED leverages only the decoded similarity to accomplish the matching process.

Different from some existing tracking-by-query methods [31], [33] that track one trajectory by using one query, in AED, the matched track queries will be updated by the corresponding object queries (dashed lines in Fig. 2). Then, the matched object queries and the unmatched track queries are treated as track queries for the next frame. Note that we do not perform matching at the end of the first frame because no track query exists at that time.

To maximize the consistency between training and association and also enhance the robustness of AED to generalize to unknown categories, we propose an association-centric learning mechanism (Section III-C) during training. By leveraging the sim-decoder, the association-centric learning mechanism is reflected in three aspects: spatial, temporal, and cross-clip. Specifically, we apply spatial contrastive learning to make AED better distinguish objects within one single frame, which is the precondition for cross-frame associations. Then we take a sampled video clip with n frames as the input and use temporal contrastive learning to help AED match objects with historical trajectories. This prompts AED to learn complex matching scenarios similar to the association phase. Moreover, we use cross-clip contrastive learning to improve the long-term ID consistency of AED on several frames. AED is only trained on specific categories following [13], while AED aims to associate arbitrary detections during inference, which is

different from [13].

B. Similarity Decoder

As illustrated in Fig. 3(a), we propose a similarity decoder (sim-decoder) with N layers to decode spatial, temporal, and cross-clip similarities S and weight responses W . During inference, only S_{temporal} is required to perform matching. During training, all of the S and W are the input of association-centric learning which will be discussed in Section III-C.

The input of the sim-decoder consists of three parts: object queries, track queries, and features map of the current frame. With the confidence scores available, we first encode M_t bounding boxes from frame t into object queries of size $M_t \times d_{\text{model}}$ by using sine-cosine positional encoding [26]. Similar to the inference phase, we also perform matching [38] during training to output real track queries for the next frame, while the input data is a sampled clip consisting of n frames. At the beginning of the sim-decoder, a multi-head deformable cross-attention [32] is employed to aggregate the appearance features of every object query on the feature map. Then we apply a feed-forward network to update the object queries. To help sim-decoder better locate the feature, we employ box refinement using updated object queries following [33] (omitted in Fig. 3(a) for simplicity and will be discussed in Section III-D).

Then, we utilize the updated object queries from three dimensions during training. Firstly, as shown in Fig. 3(a), they are the queries Q_1 for the proposed multi-head weight cross-attention, and the track queries are the keys K_1 . The output of multi-head weight cross-attention constitutes S_{temporal} and W_{temporal} . They are the similarities and weight responses between current object queries and track queries. Their number

of rows equals the number of object queries and the number of columns equals the number of track queries. S_{temporal} is then used for matching [38]. Secondly, they are the keys K_2 and queries Q_2 of multi-head weight self-attention to output S_{spatial} and W_{spatial} , which are similarities and weight responses among object queries from the present frame. The number of rows and columns of S_{spatial} and W_{spatial} both equals the number of object queries in the current frame. Thirdly, we store all of the output object queries from the sampled clip in a clip query buffer during training. At the end of the last frame, we take all object queries from the buffer as both keys K_3 and queries Q_3 for multi-head weight self-attention to output $S_{\text{cross-clip}}$ and $W_{\text{cross-clip}}$. They denote the similarity and weight responses among all the objects in the clip. Their number of rows and columns also equals the total number of objects. Note that the three mentioned multi-head weight attention share the same weights. All of the S and W are further used for association-centric learning and will be discussed in Sec. III-C.

We further introduce our proposed multi-head weight attention. Inspired by the "weight" concept in multi-head attention [26], our multi-head weight attention is only responsible for calculating the similarities S and weight responses W between the input keys K and queries Q . As illustrated in Fig. 3(b), we simplify the multi-head attention to specifically compute the S and W between queries and keys and abandon the concept of "value" in multi-head attention. The more similar a given pair of the key and query (e.g. from the same ID), the higher the corresponding similarity and response will be. If $K = Q$, it is called multi-head weight self-attention, otherwise, it is called cross-attention. To be specific, we linearly project K and Q for h times respectively, where h is the number of heads. For each head i , we compute the similarities S_i and the weight responses W_i between the projected queries and keys using weight attention. h weight attentions are employed for the similarity learning from different representation subspaces. For head i , its S_i and W_i can be formulated as:

$$S_i = \text{norm}(\text{linear}_i(Q)) \cdot \text{norm}(\text{linear}_i(K))^T, \quad (1)$$

$$W_i = \text{linear}_i(Q) \cdot \text{linear}_i(K)^T. \quad (2)$$

Different from [26], for S_i , we employ cosine similarity instead of dot product and softmax in our weight attention because the softmax function can only identify the relative maximum, not the absolute maximum, which is catastrophic for data association in MOT. For example, newly emerged objects should have low similarity with all historical trajectories. If softmax is used, the similarities will be comparatively high.

The results of h weight attentions are then averaged element-wise to output the final S and W for multi-head weight attention:

$$S = \max(0, \text{mean}(S_1, S_2, \dots, S_h)), \quad (3)$$

$$W = \text{mean}(W_1, W_2, \dots, W_h). \quad (4)$$

Note that for each element of S , we constrain its value within the range of [0,1].

During inference, we take the entire video sequence as the input. Instead of leveraging some prior knowledge like Kalman filter [18], we directly use the S_{temporal} from the final layer of sim-decoder as the input for the Hungarian algorithm [38] to perform matching. Again, we simply update the track query with the corresponding object query if they match successfully. Inspired by [16], we employ a very simple two-stage matching strategy. Specifically, We first associate the high-scoring boxes and then proceed to associate the low-scoring boxes. AED initiates every untracked bounding box as a new trajectory without any complex initialization procedures like [2], [13], [16].

C. Association-Centric Learning Mechanism

Based on the three sets of S and W that correspond to spatial, temporal, and cross-clip, we propose an association-centric learning mechanism to tackle the aforementioned association-learning ignorance problem and keep the extracted features robust enough to generalize to the unknown categories. The association-centric learning model the training process as a contrastive learning.

To better understand our approach, we visualize the association-centric learning in Fig. 4. The top-left panel of Fig. 4 provides an example of a sampled clip containing three frames during training. Assuming that there are four IDs in this clip, ID 1 and ID 4 are absent in frame 1 and frame 3 respectively. During training, their corresponding object queries are encoded from real detections.

For each W output by sim-decoder, we apply the embedding loss proposed in [22] to enhance the weight responses among keys and queries that share the same ID and diminish the responses from different IDs. We formulate the loss as follows:

$$\mathcal{L}_{\text{embed}}(W) = \sum_r \log[1 + \sum_{w_r^+} \sum_{w_r^-} \exp(w_r^- - w_r^+)], \quad (5)$$

where r is the index of rows in W , and each row of W represents the responses of all keys to the same query in multi-head weight attention. $w_r^+, w_r^- \in W_r$ and W_r denotes the r -th row of W . w_r^+ is the response between key and query from the same ID, and w_r^- is the response between different IDs. We further adopt focal loss [39] as the auxiliary loss based on the corresponding S :

$$\mathcal{L}_{\text{aux}}(S) = - \sum_{s^+} (1 - s^+)^{\gamma} \log(s^+) - \sum_{s^-} (s^-)^{\gamma} \log(1 - s^-), \quad (6)$$

where $s^+, s^- \in S$ and s^+ is the similarity between the same ID, s^- is the similarity between different IDs.

We argue that distinguishing different IDs within a single frame is fundamental for a tracker before cross-frame data association. Additionally, we all know that objects within a single frame are unique. Thus, we leverage W_{spatial} and S_{spatial} to enhance the spatial discriminative ability of AED. Specifically, we use $\mathcal{L}_{\text{embed}}$ and \mathcal{L}_{aux} to accomplish spatial contrastive learning:

$$\mathcal{L}_{\text{spatial}} = \sum_t (\mathcal{L}_{\text{embed}}(W_{\text{spatial}}^t) + \mathcal{L}_{\text{aux}}(S_{\text{spatial}}^t)), \quad (7)$$

where t is the frame index from the sampled clip.

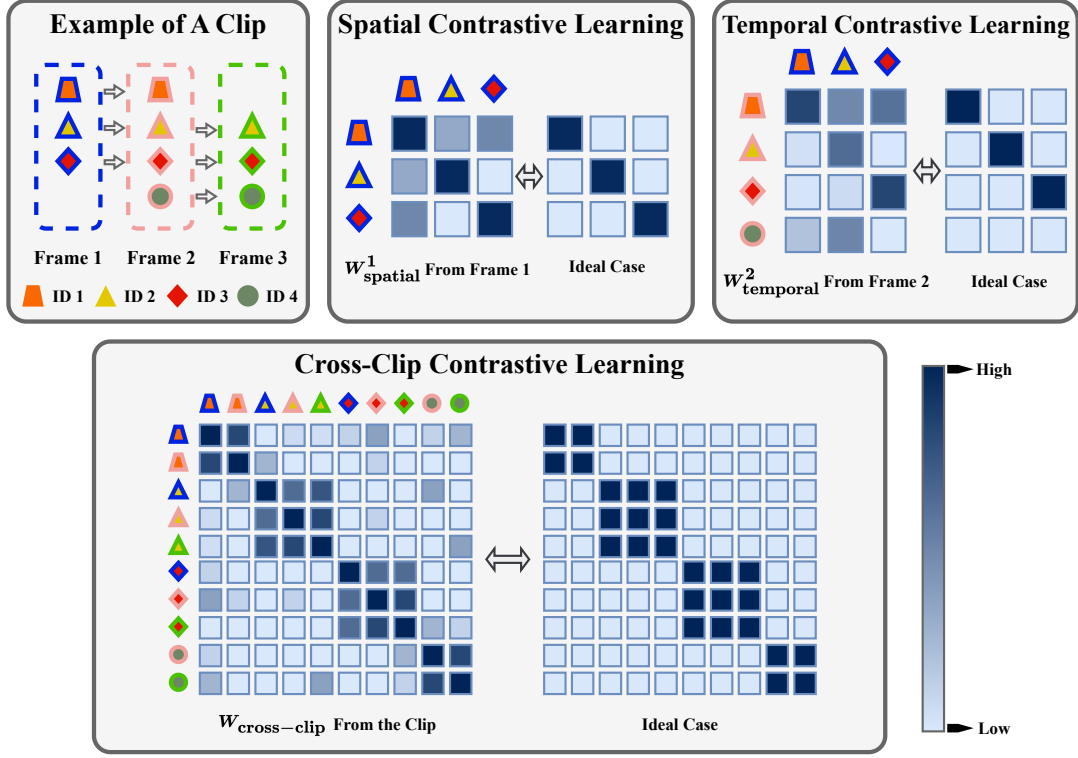


Fig. 4. Visualization of association-centric learning mechanism. It includes three aspects: spatial contrastive learning, temporal contrastive learning, and cross-clip contrastive learning.

Based on spatial contrastive learning, temporal contrastive learning aims to connect object queries with track queries that share the same ID. Again, we perform matching to achieve real track queries during training. Thus, by using W_{temporal} and S_{temporal} , temporal contrastive learning can be formulated as:

$$\mathcal{L}_{\text{temporal}} = \sum_t (\mathcal{L}_{\text{embed}}(W_{\text{temporal}}^t) + \mathcal{L}_{\text{aux}}(S_{\text{temporal}}^t)). \quad (8)$$

Since the ultimate object of MOT is to keep the ID as long as possible, we further use cross-clip contrastive learning to further intensify the long-term discriminability of AED using $W_{\text{cross-clip}}$ and $S_{\text{cross-clip}}$. Similarly, for the entire clip, we define the cross-clip contrastive learning as:

$$\mathcal{L}_{\text{cross-clip}} = \mathcal{L}_{\text{embed}}(W_{\text{cross-clip}}) + \mathcal{L}_{\text{aux}}(S_{\text{cross-clip}}). \quad (9)$$

To sum up, association-centric learning aligns the training process with the association process making AED more robust to different tracking scenarios.

D. Training Details

As mentioned in Section III-B, we refine the boxes during training. In detail, we use the object queries output by the feed-forward network in the sim-decoder and apply an additional multi-layer perceptron (MLP) to predict the compensation relative to their ground truth (GT) boxes, following [33]. The box refinement loss includes L1 loss and GIoU loss [40] denoted as \mathcal{L}_{l_1} and $\mathcal{L}_{\text{giou}}$ respectively.

As a result, our total training loss is formulated as follows:

$$\begin{aligned} \mathcal{L}_{\text{total}} = & \lambda_{\text{spatial}} \mathcal{L}_{\text{spatial}} + \lambda_{\text{temporal}} \mathcal{L}_{\text{temporal}} \\ & + \lambda_{\text{cross-clip}} \mathcal{L}_{\text{cross-clip}} + \lambda_{l_1} \mathcal{L}_{l_1} \\ & + \lambda_{\text{giou}} \mathcal{L}_{\text{giou}} \end{aligned} \quad (10)$$

where λ_{spatial} , $\lambda_{\text{temporal}}$, $\lambda_{\text{cross-clip}}$, λ_{l_1} , and λ_{giou} are the hyperparameters of their corresponding loss functions, and we set them to 0.1, 2, 1, 0.5, and 0.3 respectively. To speed up convergence and enhance the precision of the model, we also employ auxiliary losses [41] at each layer of our sim-decoder.

We use real detected boxes to generate object queries during training including the boxes that are not matched with any GT, e.g. false positives. The matched boxes (i.e. IoU with GT > 0.5) will contribute to all of the loss functions. The unmatched boxes will contribute to $\mathcal{L}_{\text{spatial}}$ and will act as negative samples in $\mathcal{L}_{\text{temporal}}$. If any object query is matched with a GT initially but its IoU with GT is smaller than a threshold τ_{iou} after box refinement, we simply filter it out to avoid ambiguous learning.

For OV-MOT tasks, we split categories into $\mathcal{C}^{\text{base}}$ and $\mathcal{C}^{\text{novel}}$ following [13]. We only use $\mathcal{C}^{\text{base}}$ to train AED, and we use $\mathcal{C}^{\text{base}}$ and $\mathcal{C}^{\text{novel}}$ to evaluate our models. For CV-MOT tasks, we utilize the entirety of the annotated data for training.

IV. EXPERIMENTS

A. Datasets And Evaluation Metrics

Datasets. We use TAO [34], DanceTrack [9], and SportsMOT [25] datasets to evaluate both OV-MOT and CV-MOT performance of AED. TAO is a large-scale dataset

TABLE I

COMPARISON WITH STATE-OF-THE-ART OV-MOT TRACKERS ON TAO DATASET. WE CATEGORIZE THE EXPERIMENTAL RESULTS BASED ON THE DIFFERENCES IN DETECTORS. "INTERGRATED" INDICATES THIS METHOD USES ITS MODEL TO LOCALIZE AND EXTRACT FEATURES OF OBJECTS SIMULTANEOUSLY. THE BEST RESULTS ARE SHOWN IN **BOLD** AND THE SECOND BEST RESULTS ARE SHOWN WITH UNDERLINES.

Detector	Method		Base				Novel			
	Validation set	Publication	TETA \uparrow	LocA \uparrow	AssocA \uparrow	ClsA \uparrow	TETA \uparrow	LocA \uparrow	AssocA \uparrow	ClsA \uparrow
Integrated	QDTrack [22]	CVPR2021	27.1	45.6	24.7	11.0	22.5	42.7	24.4	0.4
	TETer [42]	ECCV2022	30.3	47.4	31.6	12.1	25.7	45.9	31.1	0.2
	OVTrack [13]	CVPR2023	35.5	49.3	36.9	20.2	27.8	48.8	33.6	1.5
GroundingDINO [12]	NetTrack [15]	CVPR2024	33.0	45.7	28.6	24.8	32.6	51.3	33.0	13.3
RegionCLIP [11]	DeepSORT [2]	ICIP2017	28.4	52.5	15.6	17.0	24.5	49.2	15.3	9.0
	ByteTrack [16]	ECCV2022	29.4	52.3	19.8	16.0	26.5	50.8	20.9	8.0
	Tracktor++ [43]	ICCV2019	29.6	52.4	19.6	16.9	25.7	50.1	18.9	8.1
	OVTrack [13]	CVPR2023	36.3	53.9	36.3	18.7	32.0	51.4	33.2	11.4
	AED	Ours	37.3	56.4	38.4	17.0	34.4	55.9	38.5	8.7
Co-DETR [35]	DeepSORT [2]	ICIP2017	45.8	<u>70.5</u>	28.1	38.9	42.2	72.7	29.0	24.7
	ByteTrack [16]	ECCV2022	41.0	62.3	15.9	<u>44.8</u>	37.2	65.9	17.0	28.7
	OVTrack [13]	CVPR2023	<u>54.5</u>	70.3	<u>47.5</u>	45.6	<u>49.1</u>	<u>73.7</u>	<u>46.3</u>	27.2
	AED	Ours	55.7	71.5	52.2	43.5	51.4	74.4	51.8	<u>28.1</u>
Detector	Test set	Publication	TETA \uparrow	LocA \uparrow	AssocA \uparrow	ClsA \uparrow	TETA \uparrow	LocA \uparrow	AssocA \uparrow	ClsA \uparrow
Integrated	QDTrack [22]	CVPR2021	25.8	43.2	23.5	10.6	20.2	39.7	20.9	0.2
	TETer [42]	ECCV2022	29.2	44.0	30.4	10.7	21.7	39.1	25.9	0.0
	OVTrack [13]	CVPR2023	32.6	45.6	35.4	16.9	24.1	41.8	28.7	1.8
RegionCLIP [11]	DeepSORT [2]	ICIP2017	27.0	49.8	15.1	16.1	18.7	41.8	9.1	5.2
	Tracktor++ [43]	ICCV2019	28.0	49.4	18.8	15.7	20.0	42.4	12.0	5.7
	ByteTrack [16]	ECCV2022	28.7	51.5	19.9	14.5	20.4	43.0	13.5	4.9
	OVTrack [13]	CVPR2023	34.8	51.1	36.1	17.3	25.7	44.8	26.2	6.1
	AED	Ours	37.2	55.7	40.4	15.6	27.8	48.5	29.1	5.9
Co-DETR [35]	DeepSORT [2]	ICIP2017	45.6	<u>69.7</u>	30.3	36.9	41.1	<u>70.3</u>	27.8	<u>25.1</u>
	ByteTrack [16]	ECCV2022	38.8	60.6	14.8	<u>41.1</u>	31.4	55.4	15.1	23.7
	OVTrack [13]	CVPR2023	<u>53.6</u>	69.5	<u>49.3</u>	42.1	<u>45.9</u>	66.0	<u>45.3</u>	26.3
	AED	Ours	54.8	70.6	54.1	39.9	48.9	70.5	51.8	24.6

that contains 482 categories for MOT tasks. It is annotated under the federated protocol [44], and there are up to 10 labeled objects in every video of TAO. Additionally, TAO is annotated at a quite low frame rate, i.e. 1 FPS. SportsMOT aims to track players on the court, including basketball, volleyball, and football. Except for similar appearances, SportsMOT also has fast and variable-speed motion, which poses a higher challenge to the performance of the tracker. DanceTrack also has one category: person. It is a challenging dataset with diverse motion and severe occlusion, and people in DanceTrack also have very similar appearances.

Evaluation Metrics. AED can apply to both OV-MOT and CV-MOT tasks. Therefore, we use Tracking-Every-Thing Accuracy (TETA) [42] when comparing AED with other OV-MOT trackers. For CV-MOT tasks, i.e., DanceTrack and SportsMOT, we take HOTA [45], MOTA [46], and IDF1 [47] as the main evaluation metrics.

B. Implementation Details

By default, we use ResNet50 [37] as the CNN backbone of AED, and we have 6 layers of encoder and sim-decoder. We initialize AED with the Deformable DETR [32] parameters pretrained on the COCO dataset [48]. We use AdamW optimizer [49] to train AED for 5 epochs on a single RTX 4090 GPU. The initial learning rate is 1×10^{-4} , and it decreases by a factor of 10 every 2 epochs. Each batch consists of a

clip sampled from a video sequence. We set the number of sampled frames n in a clip to be 5. The d_{model} is set to 256. For the multi-head weight attention, h is set to 2.

We assign each detection box to a GT box based on an IoU threshold (> 0.5) during the clip sampling process. Since the TAO dataset is annotated under the federated protocol [44], i.e., not all instances of the same category are annotated in the images, the treatment of these unmatched boxes follows Section III-D.

During inference, we do not perform box refinement for OV-MOT tasks to avoid inaccurate refinement for the unseen $\mathcal{C}^{\text{novel}}$. The output categories are directly inherited from the detector.

C. Comparison With OV-MOT Trackers

In Tab. I, we give the evaluation result on both validation and test sets of TAO following [13]. AED is trained on $\mathcal{C}^{\text{base}}$ categories on TAO and the object queries are generated from Co-DETR [35]. During inference, we use two off-the-shelf detectors, RegionCLIP (RN50 backbone version) [11] and Co-DETR [35], to provide bounding boxes for AED. Due to the categories of the TAO dataset are consistent with those of LVIS, RegionCLIP and Co-DETR are both trained on LVIS [44].

When using RegionCLIP as the detector, AED achieves outstanding performance under the TETA metric compared with

TABLE II

COMPARISON WITH STATE-OF-THE-ART CV-MOT TRACKERS ON SPORTSMOT DATASET. METHODS IN THE GRAY BLOCKS USE THE SAME DETECTOR (YOLOX). AED* DENOTES AED IS TRAINED ON THE $\mathcal{C}^{\text{base}}$ OF TAO DATASET FOLLOWING SECTION IV-C WHILE THE TRAINING DATA OF THE DETECTOR FOLLOWS THE "TRAIN SETUP". THE BEST RESULTS ARE SHOWN IN **BOLD** AND THE SECOND BEST RESULTS ARE SHOWN WITH UNDERLINES.

Methods	Publication	Training Setup	HOTA \uparrow	IDF1 \uparrow	AssA \uparrow	MOTA \uparrow	DetA \uparrow	LocA \uparrow	IDs \downarrow
FairMOT [50]	IJCV2021	Train	49.3	53.5	34.7	86.4	70.2	83.9	9928
QDTrack [22]	CVPR2021	Train	60.4	62.3	47.2	90.1	77.5	88.0	6377
CenterTrack [51]	ECCV2020	Train	62.7	60.0	48.0	90.8	82.1	90.8	10481
TransTrack [5]	arXiv2020	Train	68.9	71.5	57.5	92.6	82.7	91.0	4992
ByteTrack [16]	ECCV2022	Train	62.8	69.8	51.2	94.1	77.1	85.6	3267
BoT-SORT [52]	arXiv2022	Train	68.7	70.0	55.9	94.5	84.4	90.5	6729
OC-SORT [17]	CVPR2023	Train	71.9	72.2	59.8	94.5	86.4	<u>92.4</u>	3093
DiffMOT [53]	CVPR2024	Train	72.1	72.8	60.5	94.5	86.0	-	-
Deep-Elou [23]	WACV2024	Train	<u>74.1</u>	75.0	<u>63.1</u>	95.1	87.2	92.5	3066
AED*	Ours	Train	72.8	<u>76.8</u>	61.4	<u>95.0</u>	86.3	92.0	2607
AED	Ours	Train	77.0	80.0	68.1	95.1	<u>87.1</u>	92.5	2240
ByteTrack [16]	ECCV2022	Train+Val	64.1	71.4	52.3	95.9	78.5	85.7	3089
MixSort-Byte [25]	ICCV2023	Train+Val	65.7	74.1	54.8	96.2	78.8	85.7	2472
OC-SORT [17]	CVPR2023	Train+Val	73.7	74.0	61.5	96.5	88.5	<u>92.7</u>	2728
MixSort-OC [25]	ICCV2023	Train+Val	74.1	74.4	62.0	96.5	88.5	<u>92.7</u>	2781
DiffMOT [53]	CVPR2024	Train+Val	76.2	76.1	65.1	97.1	<u>89.3</u>	-	-
Deep-Elou [23]	WACV2024	Train+Val	<u>77.2</u>	79.8	<u>67.7</u>	96.3	88.2	92.4	2659
AED*	Ours	Train+Val	<u>74.4</u>	78.2	<u>62.8</u>	<u>97.0</u>	88.2	92.2	<u>2250</u>
AED	Ours	Train+Val	79.1	81.8	70.1	97.1	89.4	92.8	1855

TABLE III

COMPARISON WITH STATE-OF-THE-ART CV-MOT TRACKERS ON DANCETRACK DATASET. METHODS IN THE GRAY BLOCKS USE THE SAME DETECTOR (YOLOX). AED* DENOTES AED IS TRAINED ON THE $\mathcal{C}^{\text{base}}$ OF TAO DATASET FOLLOWING SECTION IV-C. THE BEST RESULTS ARE SHOWN IN **BOLD** AND THE SECOND BEST RESULTS ARE SHOWN WITH UNDERLINES.

Methods	Publication	HOTA \uparrow	IDF1 \uparrow	AssA \uparrow	MOTA \uparrow	DetA \uparrow
Tracking-by-Detection Methods:						
FairMOT [50]	IJCV2021	39.7	40.8	23.8	82.2	66.7
CenterTrack [51]	ECCV2020	41.8	35.7	22.6	86.8	78.1
QDTrack [22]	CVPR2021	45.7	44.8	29.2	83.0	72.1
GTR [27]	CVPR2022	48.0	50.3	31.9	84.7	72.5
FineTrack [54]	CVPR2023	52.7	59.8	38.5	89.9	72.4
DeepSORT [2]	ICIP2017	45.6	47.9	29.7	87.8	71.0
ByteTrack [16]	ECCV2022	47.3	52.5	31.4	89.5	71.6
SORT [1]	ICIP2016	47.9	50.8	31.2	91.8	72.0
OC-SORT [17]	CVPR2023	54.6	54.6	40.2	89.6	80.4
DiffMOT [17]	CVPR2024	62.3	63.0	<u>47.2</u>	92.8	82.5
Hybrid-SORT [19]	AAAI2024	<u>65.7</u>	<u>67.4</u>	-	91.8	-
AED*	Ours	55.2	57.0	37.8	91.0	80.8
AED	Ours	66.6	69.7	54.3	<u>92.2</u>	<u>82.0</u>
Tracking-by-Query Methods:						
MOTR [31]	ECCV2022	54.2	51.5	40.2	79.7	73.5
SUSHI [55]	CVPR2023	63.3	63.4	50.1	88.7	80.1
MOTRv2 [33]	CVPR2022	69.9	71.7	59.0	91.9	83.0
ColTrack [28]	ICCV2023	72.6	74.0	62.3	92.1	-

several high-performance methods [2], [13], [15], [16], [22], [42], [43]. The previous state-of-the-art method OVTrack [13] uses a dual contrastive training strategy and achieves excellent performance. AED outperforms OVTrack by 2.5% (36.3%-37.2%) on TETA of base categories and 5.6% (32.0%-33.8%) on TETA of the unseen novel categories in the validation set of TAO. When it comes to the test set, AED also has an increment of 6.9% (34.8%-37.2%) on TETA of base categories and 8.2% (25.7%-27.8%) on TETA of the novel categories in the validation set of TAO. Since AED is responsible for associating every detected bounding box, the AssocA metric directly reflects the performance of AED. AED outperforms OVTrack by 4.4% (36.3%-37.9%) and 12.0% (33.2%-37.2%) on AssocA of base and novel categories of validation set

respectively. For the test set, the increment for AssocA on base and novel categories are 11.9% (36.1%-40.4%) and 11.1% (26.2%-29.1%) respectively.

Using the Co-DETR detector, AED achieves superior performance among all methods. Different from RegionCLIP, Co-DETR is a closed-vocabulary detector but AED is trained on $\mathcal{C}^{\text{base}}$ only. AED surpasses OVTrack on TETA metric by 2.2% (54.5%-55.7%) and 4.7% (49.1%-51.4%) on base and novel categories of validation set respectively, and for the test set, the increment is 2.2% (53.6%-54.8%) and 6.5% (45.9%-48.9%) respectively. AED also outperforms OVTrack in AssocA by 9.9% (47.5%-52.2%) and 11.9% (46.3%-51.8%) on base and novel categories of the validation set respectively, and in the test set, the increment is 9.7% (49.3%-54.1%) and 14.3%

TABLE IV

COMPARISON WITH STATE-OF-THE-ART TRACKERS UNDER THE CLOSED-VOCABULARY MOT SETTING ON TAO DATASET. THE BEST RESULTS ARE SHOWN IN **BOLD** AND THE SECOND BEST RESULTS ARE SHOWN WITH UNDERLINES.

Methods	Publication	TETA \uparrow	LocA \uparrow	AssocA \uparrow	ClsA \uparrow
Tracktor [43]	ICCV2019	24.2	47.4	13.0	12.1
DeepSORT [2]	ICIP2017	26.0	48.4	17.5	12.1
Tracktor++ [34]	ECCV2022	28.0	49.0	22.8	12.1
QDTrack [22]	CVPR2021	30.0	50.5	27.4	12.1
UNINEXT (R50) [56]	CVPR2023	31.9	43.3	35.5	17.1
TETer [42]	ECCV2022	33.3	51.6	35.0	13.2
OVTrack [13]	CVPR2023	34.7	49.3	36.7	18.1
GLEE-Pro [14]	CVPR2024	<u>47.2</u>	<u>66.2</u>	<u>46.2</u>	<u>29.1</u>
AED(RegionCLIP)	Ours	37.0	56.7	38.1	16.2
AED(Co-DETR)	Ours	55.3	71.8	52.4	41.7

(45.3%-51.8%).

D. Comparison With CV-MOT Trackers

We use DanceTrack [9], SportsMOT [25], and TAO [34] to evaluate the CV-MOT performance of our method.

1) *SportsMOT*: We further validate the CV-MOT performance of AED on the SportsMOT dataset. As shown in Tab II, for AED, we first use the weights trained on the $\mathcal{C}^{\text{base}}$ of TAO following Section IV-C while the detector (YOLOX [36]) is trained on the training set of SportsMOT. Under such a setting, AED achieves a competitive HOTA score, i.e. 72.8, outperforming a large number of trackers [5], [16], [17], [22], [50]–[53]. For a more equitable comparison, we also train AED, which is pretrained on COCO, on the training set of SportsMOT. AED achieves state-of-the-art performance on most metrics. Compared with Deep-ElIoU [23], AED achieves the increment of 3.9% (74.1%-77.0%) on HOTA and 6.7% (75.0%-80.0%) on IDF1 by using only training set. Note that unlike other tracking-by-detection methods leveraging some extra prior knowledge, AED only uses the similarities of features to achieve this performance.

2) *DanceTrack*: As shown in Tab. III, AED achieves the highest score in HOTA, AssA, and IDF1 metrics compared with some existing state-of-the-art tracking-by-detection CV-MOT methods. Compared with Hybrid-SORT [19], AED achieves the increment of 1.4% (65.7%-66.6%) on HOTA and 3.4% (67.4%-69.7%) on IDF1 score. The tracking-by-query CV-MOT methods like MOTRv2 [33] and ColTrack [28] achieve top-tier performance by tracking objects end-to-end. However, AED still surpasses some of the tracking-by-query methods like MOTR [31] and SUSHI [55]. When using the weights trained on the $\mathcal{C}^{\text{base}}$ of TAO following Section IV-C, AED also achieves competitive performance, i.e., 55.2 HOTA score.

3) *TAO*: We also validate the CV-MOT performance of AED on the TAO dataset. We train AED using both $\mathcal{C}^{\text{base}}$ and $\mathcal{C}^{\text{novel}}$ categories. The results are shown in Tab. IV. Using Co-DETR as the detector, AED achieves superior performance compared with existing first-class methods including GLEE [14] and OVTrack [13]. Moreover, AED also achieves competitive performance by using RegionCLIP.

TABLE V

ASSOCIATION-CENTRIC LEARNING ABLATION ON THE VALIDATION SET OF TAO DATASET.

$\mathcal{L}_{\text{spatial}}$	$\mathcal{L}_{\text{temporal}}$	$\mathcal{L}_{\text{cross-clip}}$	TETA	LocA	AssocA	ClsA
✓			39.5	70.4	6.4	41.7
	✓		55.0	71.8	51.5	41.6
		✓	53.0	71.8	45.4	41.7
	✓	✓	55.0	71.8	51.4	41.7
✓	✓		55.1	71.8	51.8	41.6
✓		✓	53.6	71.7	47.6	41.7
✓	✓	✓	55.2	71.8	52.1	41.7

TABLE VI

MULTI-HEAD WEIGHT ATTENTION ABLATION ON THE VALIDATION SET OF TAO DATASET.

h	TETA	LocA	AssocA	ClsA
1	55.1	71.8	51.8	41.7
2	55.2	71.8	52.1	41.7
4	54.8	71.8	51.0	41.7
8	55.0	71.8	51.6	41.6
16	54.6	71.7	50.5	41.7

E. Ablation Studies

In this section, we conduct several ablation experiments to analyze the impact of some components of AED.

1) *Analysis on Association-Centric Learning Mechanism*: We first verified the effectiveness of the association-centric learning mechanism on TAO in Tab. V. We conduct extensive combinations of the three proposed modules in association-centric learning. When using spatial contrastive learning ($\mathcal{L}_{\text{spatial}}$) alone, the AssocA shows a significantly low value, i.e., 6.4%. This is because spatial contrastive learning only endows AED with a sense of spatial perception. Temporal contrastive learning ($\mathcal{L}_{\text{temporal}}$) aligns with the association process because S_{temporal} is provided for data association. It can be seen from Tab. V that simply using $\mathcal{L}_{\text{temporal}}$ achieves a comparatively high TETA and AssocA. Due to an excessive focus on global consistency, utilizing only cross-clip consistency ($\mathcal{L}_{\text{cross-clip}}$) results in a suboptimal performance. With the combination of $\mathcal{L}_{\text{spatial}}$, $\mathcal{L}_{\text{temporal}}$, and $\mathcal{L}_{\text{cross-clip}}$, AED achieves the best results.

2) *Weight Attention Analysis*: In Tab. VI, we conduct several experiments to validate the impact of different h in the multi-head weight attention. We select several different values of h , i.e., 1, 2, 4, 8, and 16. It can be observed from Tab. VI that when h equals 2, the model achieves a comparatively high performance.

3) *Analysis on IoU Threshold to Filter Out Ambiguous Queries*: As introduced in Section III-D, after the refinement in training, we calculate IoUs between boxes of object queries and their GTs to filter out the ambiguous ones, i.e. $\text{IoU} < \tau_{\text{IoU}}$. In order to investigate the impact of τ_{IoU} on AED, we conduct a comparative experiment in Tab. VII. We find that a higher τ_{IoU} has a slight negative impact on the association performance (AssocA) of AED. Ultimately, we chose $\tau_{\text{IoU}} = 0.5$ during training.

4) *Analysis on the Length of Clips*: During training, we take sampled clips of n frames as the input. We conduct

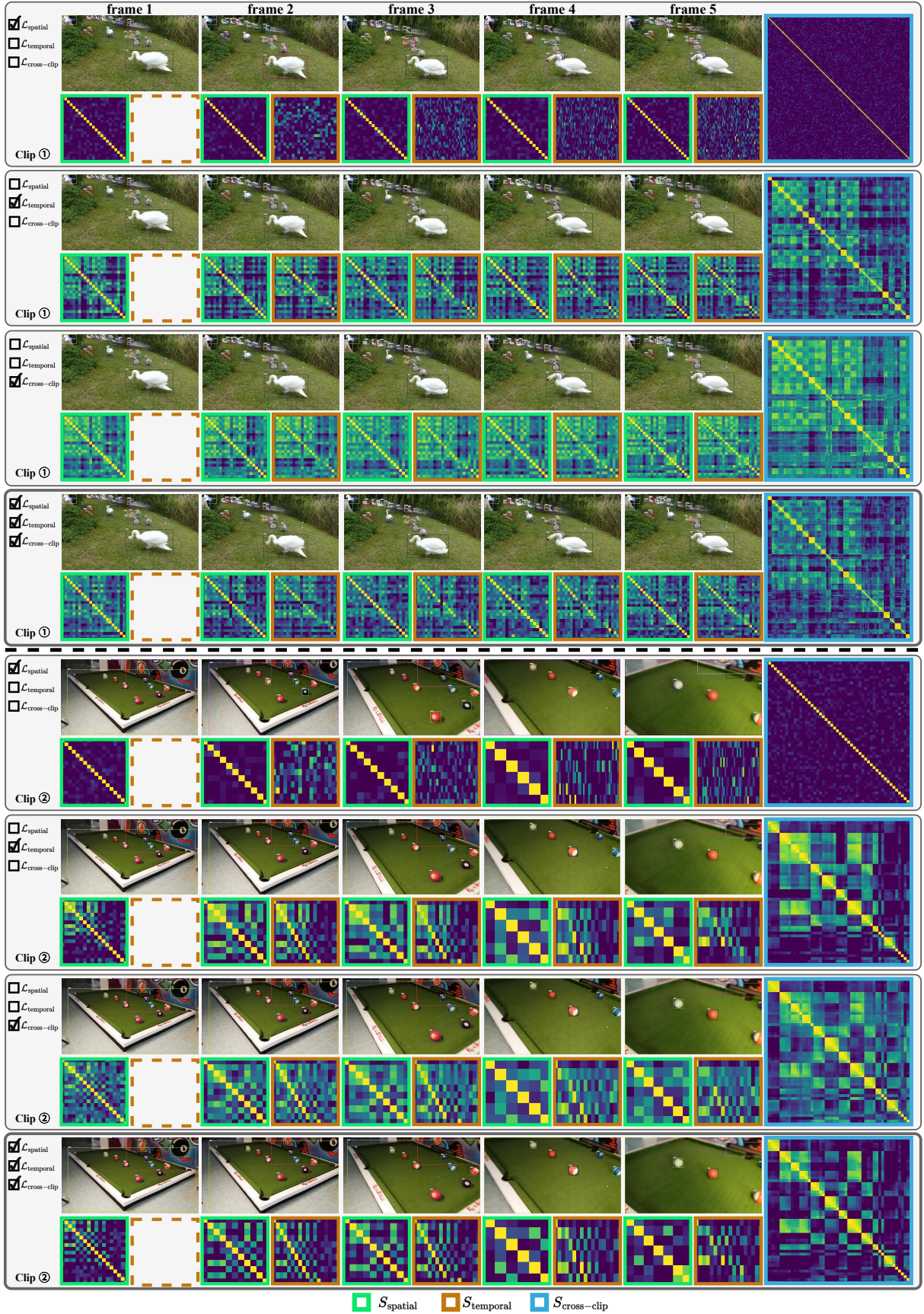


Fig. 5. Visualize the effectiveness of association-centric learning. We show spatial similarities S_{spatial} , temporal similarities S_{temporal} , and cross-clip similarities $S_{\text{cross-clip}}$ under different association-centric learning settings for clip ① and clip ②. The higher the value of each element in the S matrix, the closer its color tends to be yellow. Conversely, the closer it tends to be blue.



Fig. 6. Successful and failed cases of AED. We visualize some tracking results from TAO, SportsMOT, and DanceTrack.

TABLE VII
 τ_{iou} ABLATION ON THE VALIDATION SET OF TAO DATASET.

τ_{iou}	TETA	LocA	AssocA	ClsA
0.1	55.1	71.8	51.8	41.7
0.3	55.2	71.9	51.9	41.7
0.5	55.2	71.8	52.1	41.7
0.7	55.0	71.8	51.5	41.7
0.9	54.3	71.7	49.5	41.8

TABLE VIII
THE IMPACT OF DIFFERENT CLIP LENGTHS ON THE PERFORMANCE OF AED.

Clip Length	TETA	LocA	AssocA	ClsA
2	53.6	71.8	47.3	41.7
3	54.9	71.7	51.3	41.7
4	55.1	71.7	51.8	41.7
5	55.2	71.8	52.1	41.7

an experiment on the TAO dataset to find the most suitable n in Tab. VIII. We can find that with the increment of n , the performance of AED also improves. However, due to the limitation of GPU memory, $n = 5$ represents the current upper limit of our experimental conditions.

5) *Analysis on Sampling Strategy*: As the input of AED is a video clip in the training stage, there are different ways to merge a number of video frames into a clip. We conduct ablation experiments on two sampling methods on the TAO dataset as shown in Tab. IX. The first setting is that we fix the

sampling interval to the number of three, i.e., skip two frames when sampling. Second, we allowed the sampling interval to change randomly within the range of $[0, 3]$, which introduces a wider variety of displacement and perspective changes during training. We find that the random sampling strategy improves the AssocA by 0.6 points.

6) *Analysis on Performance Ceiling*: To further exhibit the upper limits of AED, we replace the detection boxes with GTs. We compare AED with several other high-performance methods including ByteTrack [16], DeepSORT [2], and OV-

TABLE IX
DIFFERENT SAMPLING STRATEGY ABLATION ON THE VALIDATION SET OF
TAO DATASET.

Sampling Methods	TETA	LocA	AssocA	ClsA
fixed	54.9	71.7	51.5	41.6
random	55.2	71.8	52.1	41.7

TABLE X
TO SHOW THE PERFORMANCE CEILING OF AED, WE COMPARE SEVERAL
OV-MOT TRACKERS WITH AED BY USING GT BOUNDING BOXES
DURING INFERENCE.

Methods	TETA	LocA	AssocA	ClsA
ByteTrack [16]	75.0	99.2	27.2	98.7
Deepsort [2]	75.1	96.3	33.2	95.9
OVTrack [13]	87.6	99.5	71.9	91.5
AED (Ours)	92.3	99.2	77.7	99.9

Track [13] in Tab. X. AED achieves the highest performance among TETA, AssocA, and ClsA metrics.

F. Visualization

1) *Association-Centric Learning*: In Fig. 5, we visualize the three proposed similarity matrices, i.e., S_{spatial} , S_{temporal} , and $S_{\text{cross-clip}}$, from two scenes under different settings to validate the effectiveness of association-centric learning. We arrange the rows and columns of each S in the order of the IDs. Ideally, high-response elements (yellow ones) should be along the diagonal or within the diagonal blocks. For each clip, we also visualize its tracking result and represent different IDs with bounding boxes of different colors. When only adopting spatial contrastive learning ($\mathcal{L}_{\text{spatial}}$), the model identifies every detected object as a unique ID due to the lack of temporal supervision (first row of clip ① and ②). As mentioned above, $S_{\text{cross-clip}}$ represents similarities between every collected object query in the entire clip. This can be further verified from another perspective that $S_{\text{cross-clip}}$ has no high-response block along the diagonal. Simply using temporal contrastive learning ($\mathcal{L}_{\text{temporal}}$) achieves moderately good results (second row of clip ① and ②). However, compared with the last row of each clip, some erroneous high-response regions can still be observed especially in the $S_{\text{cross-clip}}$ of clip ②. When using cross-clip contrastive learning ($\mathcal{L}_{\text{cross-clip}}$) alone, all of the elements of S_{spatial} , S_{temporal} , and $S_{\text{cross-clip}}$ in clip ① and clip ② have relatively high responses (third row of clip ① and ②). This is because of the overemphasis on global feature consistency. When making full use of association-centric learning, the discriminative ability of AED is further enhanced in the last row of clip ① and ②. We can see from S_{spatial} that AED can distinguish between each object within a single frame very well, as almost every S_{spatial} matrix exhibits high responses only along the diagonal. Also, it can be observed from the S_{temporal} matrices that nearly every track query is matched correctly even with very similar appearances in clip ①. It can be observed that almost all high-similarity blocks are exclusively found on the diagonal of $S_{\text{cross-clip}}$.

2) *Tracking Results*: In Fig. 6, we visualize some successful and failed tracking results of AED on different datasets

including TAO, SportsMOT, and DanceTrack. Specifically, we use Co-DETR in TAO and YOLOX in SportsMOT and DanceTrack. AED is able to handle a wide range of scenarios including low frame rates (TAO), large movements (SportsMOT), severe occlusions (DanceTrack), and similar appearances (SportsMOT and DanceTrack). However, AED makes some mistakes in cases involving tiny objects (ID9, 10, 12, etc of the first row of the TAO dataset) and highly dense scenes (ID 64, 65, etc of the second row of the TAO dataset).

V. CONCLUSION

In this paper, we propose AED to apply to OV-MOT and CV-MOT tasks following the tracking-by-detection paradigm. AED is compatible with various detectors and unknown categories. We employ a very simple matching strategy by using the proposed sim-decoder without any prior knowledge. Moreover, we propose association-centric learning to ensure that the training objective remains consistent with the needs of the association phase. We also conducted sufficient experiments to validate the superior performance of our method compared with existing OV-MOT and CV-MOT trackers.

However, AED also has its limitations:

- AED struggles to tackle extremely crowded scenarios due to the lack of motion cues.
- Object queries of AED are quite homogeneous, originating solely from the detector and lacking information from other forms or modalities, such as text.

REFERENCES

- [1] A. Bewley, Z. Ge, L. Ott, F. Ramos, and B. Upcroft, "Simple online and realtime tracking," in *2016 IEEE international conference on image processing (ICIP)*. IEEE, 2016, pp. 3464–3468.
- [2] N. Wojke, A. Bewley, and D. Paulus, "Simple online and realtime tracking with a deep association metric," in *2017 IEEE international conference on image processing (ICIP)*. IEEE, 2017, pp. 3645–3649.
- [3] Z. Wang, L. Zheng, Y. Liu, Y. Li, and S. Wang, "Towards real-time multi-object tracking," in *European Conference on Computer Vision*. Springer, 2020, pp. 107–122.
- [4] C. Liang, Z. Zhang, X. Zhou, B. Li, S. Zhu, and W. Hu, "Rethinking the competition between detection and reid in multiobject tracking," *IEEE Transactions on Image Processing*, vol. 31, pp. 3182–3196, 2022.
- [5] P. Sun, J. Cao, Y. Jiang, R. Zhang, E. Xie, Z. Yuan, C. Wang, and P. Luo, "Trantrack: Multiple object tracking with transformer," *arXiv preprint arXiv:2012.15460*, 2020.
- [6] L. Leal-Taixé, A. Milan, I. Reid, S. Roth, and K. Schindler, "Motchallenge 2015: Towards a benchmark for multi-target tracking," *arXiv preprint arXiv:1504.01942*, 2015.
- [7] A. Milan, L. Leal-Taixé, I. Reid, S. Roth, and K. Schindler, "Mot16: A benchmark for multi-object tracking," *arXiv preprint arXiv:1603.00831*, 2016.
- [8] P. Dendorfer, H. Rezatofighi, A. Milan, J. Shi, D. Cremers, I. Reid, S. Roth, K. Schindler, and L. Leal-Taixé, "Mot20: A benchmark for multi object tracking in crowded scenes," *arXiv preprint arXiv:2003.09003*, 2020.
- [9] P. Sun, J. Cao, Y. Jiang, Z. Yuan, S. Bai, K. Kitani, and P. Luo, "Dancetrack: Multi-object tracking in uniform appearance and diverse motion," in *Proceedings of the IEEE/CVF Conference on Computer Vision and Pattern Recognition*, 2022, pp. 20993–21002.
- [10] A. Radford, J. W. Kim, C. Hallacy, A. Ramesh, G. Goh, S. Agarwal, G. Sastry, A. Askell, P. Mishkin, J. Clark *et al.*, "Learning transferable visual models from natural language supervision," in *International conference on machine learning*. PMLR, 2021, pp. 8748–8763.
- [11] Y. Zhong, J. Yang, P. Zhang, C. Li, N. Codella, L. H. Li, L. Zhou, X. Dai, L. Yuan, Y. Li *et al.*, "Regionclip: Region-based language-image pretraining," in *Proceedings of the IEEE/CVF Conference on Computer Vision and Pattern Recognition*, 2022, pp. 16793–16803.

- [12] S. Liu, Z. Zeng, T. Ren, F. Li, H. Zhang, J. Yang, C. Li, J. Yang, H. Su, J. Zhu *et al.*, “Grounding dino: Marrying dino with grounded pre-training for open-set object detection,” *arXiv preprint arXiv:2303.05499*, 2023.
- [13] S. Li, T. Fischer, L. Ke, H. Ding, M. Danelljan, and F. Yu, “Ov-track: Open-vocabulary multiple object tracking,” in *Proceedings of the IEEE/CVF Conference on Computer Vision and Pattern Recognition*, 2023, pp. 5567–5577.
- [14] J. Wu, Y. Jiang, Q. Liu, Z. Yuan, X. Bai, and S. Bai, “General object foundation model for images and videos at scale,” *arXiv preprint arXiv:2312.09158*, 2023.
- [15] G. Zheng, S. Lin, H. Zuo, C. Fu, and J. Pan, “Nettrack: Tracking highly dynamic objects with a net,” *arXiv preprint arXiv:2403.11186*, 2024.
- [16] Y. Zhang, P. Sun, Y. Jiang, D. Yu, F. Weng, Z. Yuan, P. Luo, W. Liu, and X. Wang, “Bytetrack: Multi-object tracking by associating every detection box,” in *European Conference on Computer Vision*. Springer, 2022, pp. 1–21.
- [17] J. Cao, J. Pang, X. Weng, R. Khrodar, and K. Kitani, “Observation-centric sort: Rethinking sort for robust multi-object tracking,” in *Proceedings of the IEEE/CVF Conference on Computer Vision and Pattern Recognition*, 2023, pp. 9686–9696.
- [18] R. E. Kalman, “A new approach to linear filtering and prediction problems,” *Journal of Basic Engineering*, vol. 82, no. 1, pp. 35–45, 03 1960. [Online]. Available: <https://doi.org/10.1115/1.3662552>
- [19] M. Yang, G. Han, B. Yan, W. Zhang, J. Qi, H. Lu, and D. Wang, “Hybrid-sort: Weak cues matter for online multi-object tracking,” in *Proceedings of the AAAI Conference on Artificial Intelligence*, vol. 38, no. 7, 2024, pp. 6504–6512.
- [20] J. Seidenschwarz, G. Brasó, V. C. Serrano, I. Elezi, and L. Leal-Taixé, “Simple cues lead to a strong multi-object tracker,” in *Proceedings of the IEEE/CVF Conference on Computer Vision and Pattern Recognition*, 2023, pp. 13 813–13 823.
- [21] A. Hermans, L. Beyer, and B. Leibe, “In defense of the triplet loss for person re-identification,” *arXiv preprint arXiv:1703.07737*, 2017.
- [22] J. Pang, L. Qiu, X. Li, H. Chen, Q. Li, T. Darrell, and F. Yu, “Quasi-dense similarity learning for multiple object tracking,” in *Proceedings of the IEEE/CVF conference on computer vision and pattern recognition*, 2021, pp. 164–173.
- [23] H.-W. Huang, C.-Y. Yang, J. Sun, P.-K. Kim, K.-J. Kim, K. Lee, C.-I. Huang, and J.-N. Hwang, “Iterative scale-up expansion and deep features association for multi-object tracking in sports,” in *Proceedings of the IEEE/CVF Winter Conference on Applications of Computer Vision*, 2024, pp. 163–172.
- [24] J. Redmon and A. Farhadi, “Yolov3: An incremental improvement,” *arXiv preprint arXiv:1804.02767*, 2018.
- [25] Y. Cui, C. Zeng, X. Zhao, Y. Yang, G. Wu, and L. Wang, “Sportsmot: A large multi-object tracking dataset in multiple sports scenes,” in *Proceedings of the IEEE/CVF International Conference on Computer Vision*, 2023, pp. 9921–9931.
- [26] A. Vaswani, N. Shazeer, N. Parmar, J. Uszkoreit, L. Jones, A. N. Gomez, Ł. Kaiser, and I. Polosukhin, “Attention is all you need,” *Advances in neural information processing systems*, vol. 30, 2017.
- [27] X. Zhou, T. Yin, V. Koltun, and P. Krähenbühl, “Global tracking transformers,” in *Proceedings of the IEEE/CVF Conference on Computer Vision and Pattern Recognition*, 2022, pp. 8771–8780.
- [28] Y. Liu, J. Wu, and Y. Fu, “Collaborative tracking learning for frame-rate-insensitive multi-object tracking,” in *Proceedings of the IEEE/CVF International Conference on Computer Vision*, 2023, pp. 9964–9973.
- [29] J. Cai, M. Xu, W. Li, Y. Xiong, W. Xia, Z. Tu, and S. Soatto, “Memot: Multi-object tracking with memory,” in *Proceedings of the IEEE/CVF Conference on Computer Vision and Pattern Recognition*, 2022, pp. 8090–8100.
- [30] R. Gao and L. Wang, “Memotr: Long-term memory-augmented transformer for multi-object tracking,” in *Proceedings of the IEEE/CVF International Conference on Computer Vision*, 2023, pp. 9901–9910.
- [31] F. Zeng, B. Dong, Y. Zhang, T. Wang, X. Zhang, and Y. Wei, “Motr: End-to-end multiple-object tracking with transformer,” in *European Conference on Computer Vision*. Springer, 2022, pp. 659–675.
- [32] X. Zhu, W. Su, L. Lu, B. Li, X. Wang, and J. Dai, “Deformable detr: Deformable transformers for end-to-end object detection,” *arXiv preprint arXiv:2010.04159*, 2020.
- [33] Y. Zhang, T. Wang, and X. Zhang, “Motrv2: Bootstrapping end-to-end multi-object tracking by pretrained object detectors,” in *Proceedings of the IEEE/CVF Conference on Computer Vision and Pattern Recognition*, 2023, pp. 22 056–22 065.
- [34] A. Dave, T. Khurana, P. Tokmakov, C. Schmid, and D. Ramanan, “Tao: A large-scale benchmark for tracking any object,” in *Computer Vision–ECCV 2020: 16th European Conference, Glasgow, UK, August 23–28, 2020, Proceedings, Part V 16*. Springer, 2020, pp. 436–454.
- [35] Z. Zong, G. Song, and Y. Liu, “Detrs with collaborative hybrid assignments training,” in *Proceedings of the IEEE/CVF international conference on computer vision*, 2023, pp. 6748–6758.
- [36] Z. Ge, S. Liu, F. Wang, Z. Li, and J. Sun, “Yolox: Exceeding yolo series in 2021,” *arXiv preprint arXiv:2107.08430*, 2021.
- [37] K. He, X. Zhang, S. Ren, and J. Sun, “Deep residual learning for image recognition,” in *Proceedings of the IEEE conference on computer vision and pattern recognition*, 2016, pp. 770–778.
- [38] J. Munkres, “Algorithms for the assignment and transportation problems,” *Journal of the society for industrial and applied mathematics*, vol. 5, no. 1, pp. 32–38, 1957.
- [39] T.-Y. Lin, P. Goyal, R. Girshick, K. He, and P. Dollár, “Focal loss for dense object detection,” in *Proceedings of the IEEE international conference on computer vision*, 2017, pp. 2980–2988.
- [40] H. Rezatofighi, N. Tsoi, J. Gwak, A. Sadeghian, I. Reid, and S. Savarese, “Generalized intersection over union: A metric and a loss for bounding box regression,” in *Proceedings of the IEEE/CVF conference on computer vision and pattern recognition*, 2019, pp. 658–666.
- [41] R. Al-Rfou, D. Choe, N. Constant, M. Guo, and L. Jones, “Character-level language modeling with deeper self-attention,” in *Proceedings of the AAAI conference on artificial intelligence*, vol. 33, no. 01, 2019, pp. 3159–3166.
- [42] S. Li, M. Danelljan, H. Ding, T. E. Huang, and F. Yu, “Tracking every thing in the wild,” in *European Conference on Computer Vision*. Springer, 2022, pp. 498–515.
- [43] P. Bergmann, T. Meinhardt, and L. Leal-Taixé, “Tracking without bells and whistles,” in *Proceedings of the IEEE/CVF International Conference on Computer Vision*, 2019, pp. 941–951.
- [44] A. Gupta, P. Dollar, and R. Girshick, “Lvis: A dataset for large vocabulary instance segmentation,” in *Proceedings of the IEEE/CVF conference on computer vision and pattern recognition*, 2019, pp. 5356–5364.
- [45] J. Luiten, A. Osep, P. Dendorfer, P. Torr, A. Geiger, L. Leal-Taixé, and B. Leibe, “Hota: A higher order metric for evaluating multi-object tracking,” *International journal of computer vision*, vol. 129, pp. 548–578, 2021.
- [46] K. Bernardin and R. Stiefelhagen, “Evaluating multiple object tracking performance: the clear mot metrics,” *EURASIP Journal on Image and Video Processing*, vol. 2008, pp. 1–10, 2008.
- [47] E. Ristani, F. Solera, R. Zou, R. Cucchiara, and C. Tomasi, “Performance measures and a data set for multi-target, multi-camera tracking,” in *European conference on computer vision*. Springer, 2016, pp. 17–35.
- [48] T.-Y. Lin, M. Maire, S. Belongie, J. Hays, P. Perona, D. Ramanan, P. Dollár, and C. L. Zitnick, “Microsoft coco: Common objects in context,” in *Computer Vision–ECCV 2014: 13th European Conference, Zurich, Switzerland, September 6–12, 2014, Proceedings, Part V 13*. Springer, 2014, pp. 740–755.
- [49] I. Loshchilov and F. Hutter, “Decoupled weight decay regularization,” *arXiv preprint arXiv:1711.05101*, 2017.
- [50] Y. Zhang, C. Wang, X. Wang, W. Zeng, and W. Liu, “Fairmot: On the fairness of detection and re-identification in multiple object tracking,” *International Journal of Computer Vision*, vol. 129, pp. 3069–3087, 2021.
- [51] X. Zhou, V. Koltun, and P. Krähenbühl, “Tracking objects as points,” in *European conference on computer vision*. Springer, 2020, pp. 474–490.
- [52] N. Aharon, R. Orfaig, and B.-Z. Bobrovsky, “Bot-sort: Robust associations multi-pedestrian tracking,” *arXiv preprint arXiv:2206.14651*, 2022.
- [53] W. Lv, Y. Huang, N. Zhang, R.-S. Lin, M. Han, and D. Zeng, “Diffmot: A real-time diffusion-based multiple object tracker with non-linear prediction,” in *Proceedings of the IEEE/CVF Conference on Computer Vision and Pattern Recognition*, 2024, pp. 19 321–19 330.
- [54] H. Ren, S. Han, H. Ding, Z. Zhang, H. Wang, and F. Wang, “Focus on details: Online multi-object tracking with diverse fine-grained representation,” in *Proceedings of the IEEE/CVF Conference on Computer Vision and Pattern Recognition*, 2023, pp. 11 289–11 298.
- [55] O. Cetintas, G. Brasó, and L. Leal-Taixé, “Unifying short and long-term tracking with graph hierarchies,” in *Proceedings of the IEEE/CVF Conference on Computer Vision and Pattern Recognition*, 2023, pp. 22 877–22 887.
- [56] B. Yan, Y. Jiang, J. Wu, D. Wang, P. Luo, Z. Yuan, and H. Lu, “Universal instance perception as object discovery and retrieval,” in *Proceedings of the IEEE/CVF Conference on Computer Vision and Pattern Recognition*, 2023, pp. 15 325–15 336.